



Molecular structure (monomeric and dimeric structure) and HOMO–LUMO analysis of 2-aminonicotinic acid: A comparison of calculated spectroscopic properties with FT-IR and UV–vis

Mehmet Karabacak^a, Etem Kose^b, Ahmet Atac^{b,*}

^a Department of Physics, Afyon Kocatepe University, Afyonkarahisar, Turkey

^b Department of Physics, Celal Bayar University, Manisa, Turkey

ARTICLE INFO

Article history:

Received 4 December 2011

Received in revised form 19 January 2012

Accepted 30 January 2012

Keywords:

2-Aminonicotinic acid

UV–vis and FT-IR spectra

DFT

Intermolecular hydrogen bond

ABSTRACT

The experimental (UV–vis and FT-IR) and theoretical study of 2-aminonicotinic acid ($C_6H_6N_2O_2$) was presented in this work. The ultraviolet absorption spectrum of title molecule that dissolved in ethanol and water were examined in the range of 200–400 nm. The FT-IR spectrum of the title molecule in the solid state were recorded in the region of 400–4000 cm^{-1} . The geometrical parameters and energies of 2-aminonicotinic acid have been obtained for all four conformers/isomers (C1, C2, C3, C4) from DFT (B3LYP) with 6-311++G(d,p) basis set calculations. C1 form has been identified the most stable conformer due to computational results. Therefore, spectroscopic properties have been searched for the most stable form of the molecule. The vibrational frequencies were calculated and scaled values were compared with experimental FT-IR spectrum. The complete assignments were performed based on the total energy distribution (TED) of the vibrational modes, calculated with scaled quantum mechanics (SQM) method. Also the molecular structures, vibrational frequencies, infrared intensities were calculated for a pair of molecules linked by the intermolecular O–H...O hydrogen bond. Moreover, the thermodynamic properties of the studied compound at different temperatures were calculated. Besides, charge transfer occurring in the molecule between HOMO and LUMO energies, frontier energy gap, molecular electrostatic potential (MEP) were calculated and presented. The spectroscopic and theoretical results are compared to the corresponding properties for monomer and dimer of C1 conformer. The optimized bond lengths, bond angles, calculated frequencies and electronic transitions showed the agreement with the experimental results.

© 2012 Elsevier B.V. All rights reserved.

1. Introduction

Nicotinic acid (also known as niacin, pyridine-3-carboxylic acid, vitamin B3) and its derivatives have been subjected to many types of scientific studies via its importance. Nicotinic acid is a valuable chemical product and an important vitamin of B group. It is widely used in medicine, in food industry, in agriculture, and in production of cosmetics. Annual worldwide output of nicotinic acid is ca. 35,000 ton [1]. 2-Aminonicotinic acid is a derivative of pyridine, with a carboxyl group (COOH) at the 3-position and an amino group (NH₂) at the 2-position.

Nicotinic acid and its derivatives have recently become attractive to experimentalists as well as theoreticians since their structures are of some biological significance particularly in medicinal and cosmetic chemistry [2–17]. Extensive experimental and theoretical

investigations have focused on elucidating the structure and normal vibrations of nicotinic acid derivatives. Koczoń et al. [2] studied the experimental and theoretical vibrational spectra of picolinic, nicotinic and isonicotinic acids. The nicotinic acid and its complexes with different metals were researched with different methods [3,4]. Matthew et al. [5] characterized the vibrational spectrum of nicotinic acid in the solid-state. X-ray absorption spectroscopy (XAS) and scanning tunneling microscopy (STM) have been used to study the absorption of monolayers of the pyridinecarboxylic acid monomers (isonicotinic acid, nicotinic acid, and picolinic acid) and benzoic acid on a rutile TiO₂ (1 1 0) surface by Schnadt et al. [6]. Polymeric lanthanide (III) complexes of nicotinic acid N-oxide and isonicotinic acid N-oxide have been synthesized and structurally determined by Jiang-Gao Mao et al. [7]. Goher et al. [8] described the synthesis and crystal structures of two new lanthanide complexes of isonicotinic acid N-oxide. The geometry of 2-(2-methyl-3-chloroanilino) nicotinic acid was studied in the gas phase and in the solid state using ab initio Hartree–Fock methods by Franckaerts et al. [9]. Cobb et al. [10] investigated metabolism of

* Corresponding author. Tel.: +90 236 241 2151.

E-mail address: ahmet.atac@bayar.edu.tr (A. Atac).

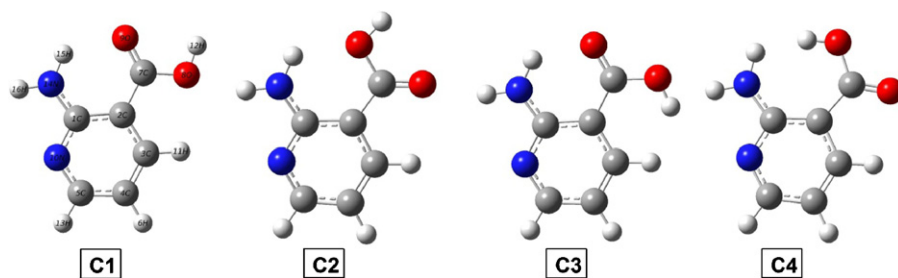


Fig. 1. The theoretical geometric structures of 2-ANA.

6-aminonicotinic acid in *Escherichia coli*. The feasibility of electro-synthesis of 6-aminonicotinic acid by electrochemical reduction of 2-amino-5-bromo and 2-amino-5-chloropyridine in the presence of CO₂ was investigated in DMF and CH₃CN at glassy carbon (GC), Hg, Pt and Ag electrodes by Gennaro et al. [11]. Nayak and Dogra [12] carried out absorption, fluorescence excitation and fluorescence spectroscopic, as well as time-correlated single-photon studies on 6-aminonicotinic acid in different solvents and acid–base concentration. Soares-Santos et al. [13] synthesized terbium (III) complexes of 2-aminonicotinic, thio-salicylic and anthranilic acids and investigated photoluminescence properties. Dogra [14] investigated absorption, fluorescence excitation and fluorescence spectroscopy combined with time-dependent spectrofluorimetry to study the effect of solvents and acid–base concentration on the spectral characteristics of 2-aminonicotinic acid. The influence of lithium, sodium, potassium, rubidium and cesium on the electronic system of 2-aminonicotinic acid was studied by the methods of molecular spectroscopy by Świsłocka et al. [15]. The experimental and theoretical study on the structures and vibrations of 2- and 6-chloronicotinic acid were presented [16,17]. Karabacak et al. [18] recorded the FT-IR and FT-Raman spectrum and presented the detailed vibrational assignment for 2-bromonicotinic acid and 6-bromonicotinic acid.

The geometric structures of 2-aminonicotinic acid (abbreviated henceforth 2-ANA) were studied by X-ray [19]. In this case, the aim of this study is to fully determine the molecular structure, vibrational modes and wavenumbers and absorption bands of 2-ANA experimentally (FT-IR and UV–vis spectrum) and theoretically. For computations we have carried out DFT calculations with the combined Becke's three-parameter exchange functional in combination with the Lee, Yang and Parr correlation functional (B3LYP). All calculations have been studied for C1 form and C1 dimer of 2-ANA. These calculations are valuable for providing insight into the vibrational spectrum and the geometric structure, vibrational energies, absorption wavelengths, excitation energies and electric dipole moment (μ) of 2-ANA. Detailed interpretations of the vibrational spectra of 2-ANA have been made on the basis of the calculated total energy distribution (TED).

2. Experimental

The compound 2-ANA in solid state was purchased from Across Organics Company with a stated purity of 99%. The FT-IR spectrum of 2-ANA molecule was recorded between 4000 and 400 cm⁻¹ on a Perkin–Elmer FT-IR System Spectrum BX spectrometer, which was calibrated using polystyrene bands. The spectrum was recorded at room temperature with a scanning speed of 10 cm⁻¹ min⁻¹ and the spectral resolution of 4.0 cm⁻¹. The ultraviolet absorption spectrum of 2-ANA solved in ethanol and water were examined in the range of 200–400 nm using Shimadzu UV-2401 PC, UV–vis recording Spectrometer. Data were analyzed by UV PC Personal Spectroscopy Software, version 3.91.

3. Computational details

The first task for the computational work was to determine the optimized geometry of the compound. The hybrid B3LYP [20,21] method based on Becke's three parameter functional of DFT and 6-311++G(d,p) basis set level was chosen. Optimized structural parameters were used in the vibrational frequency, isotropic chemical shift and calculations of electronic properties. However, the frequency values computed at this level contains known systematic errors [22]. Therefore, it is customary to scale down the calculated harmonic frequencies in order to improve the agreement with the experiment. In our study, we have followed two different scaling factors, i.e. 0.983 up to 1700 cm⁻¹ and 0.958 for greater than 1700 cm⁻¹ [23]. Analytic frequency calculations at the optimized geometry were done to confirm the optimized structures to be an energy minimum and to obtain the theoretical vibrational spectra. The stability of the optimized geometries was confirmed by frequency calculations, which give positive values for all obtained frequencies. All calculations were performed by using the Gaussian 03 program package on a personal computer [24]. The total energy distribution (TED) was calculated by using the scaled quantum mechanics (SQM) method and PQS program [25,26] and the fundamental vibrational modes were characterized by their TED.

The time dependent DFT (TD-DFT) proved to be a powerful and effective computational tool for the study of ground and excited state properties by comparison to the available experimental data. Hence, we used TD-B3LYP to obtain wavelengths λ_{\max} and compare with the experimental UV–vis absorption spectra of 2-ANA.

4. Results and discussion

The molecule of 2-ANA, which has two substituents such that the amide group (NH₂) and carboxyl acid group (COOH), attached to a planar pyridine ring. All forms of the molecule, amide group, carboxyl acid group and pyridine ring are in the same plane. In connection with the hydrogen orientations of the oxygen atom of the carboxylic acid group, 2-ANA has four different possible structures. The atomic numbering scheme of most stable conformer, other conformers and dimer structure of title sample shown in Figs. 1 and 2 contain two intermolecular and two intramolecular hydrogen bonds. We reported geometric parameters, vibrational frequencies and absorption wavelengths for 2-ANA by using DFT/B3LYP and compared with the experimental crystal geometries (bond lengths, bond angles) [19], experimental infrared frequencies and absorption wavelengths.

4.1. Energetics

The calculated energies and energy difference for all conformers of 2-ANA, determined by DFT/B3LYP/6-311++G(d,p) are presented in Table 1. Intra-hydrogen bonds can be responsible for the geometry and the stability of a predominant conformation; the formation

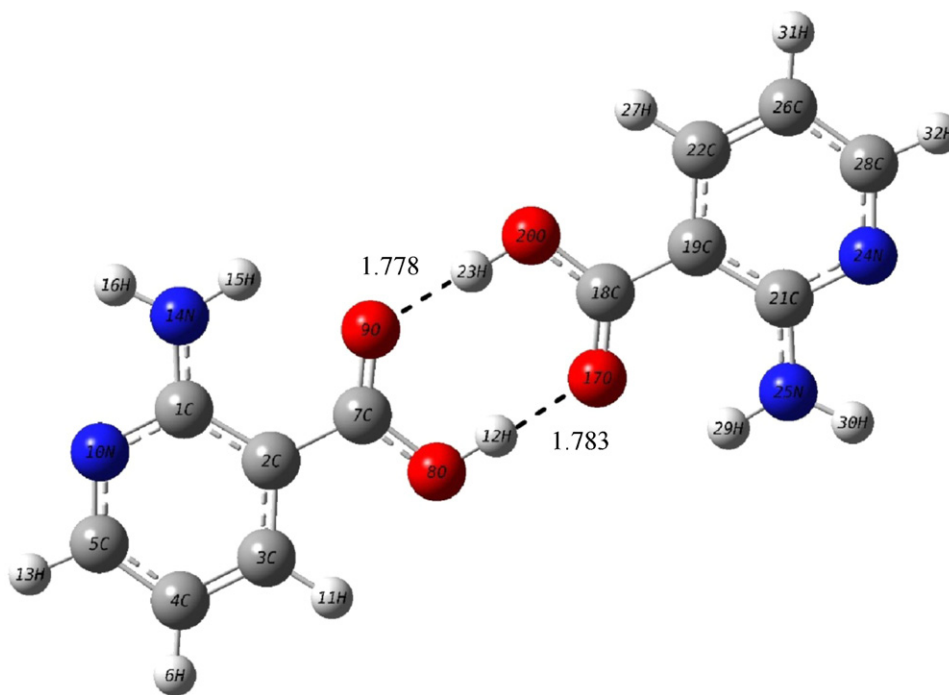


Fig. 2. C1 dimer conformer of 2-ANA in the gas phase.

of hydrogen bonding between a hydroxyl group and O=COH cause the structure of the conformer C1 to be the most stable conformer for 2-ANA. Additionally, the calculations showed that the conformer C4 to be the least stable conformer as shown in Table 1. Using the energy of the lowest energy (C1) as reference point, the relative energy of the other conformers was as: $\Delta E = E(C_n) - E(C1)$. All the relative quantities of ΔE energies related to C1 and C4 are given in Table 1 for comparison. From DFT calculations of conformers with 6-311++G(d,p) basis set, the conformer C1 is predicted to be from 0.0043 to 0.0305 kcal mol⁻¹ more stable than the other conformers of our title molecule. C1 and C2 conformers are calculated to have higher energies than the other conformers, even though there might exist weaker hydrogen bonding either between the O–H group and the O atom which COOH group or between the H atoms which COOH group and the O–H group for our title molecule.

4.2. Molecular geometry and potential energy surface scan

The molecular structure of 2-ANA molecule has been studied by X-ray diffraction [19]. Firstly, the computational work determined the optimized geometry for four conformer. The optimized geometrical parameters has minimum energy, is compared the X-ray study. The determination structure for the ground state shows that amide and carboxylic group is parallel to ring plane. The predicted bond lengths, bond angles and selected dihedral angles for most stable conformer (C1) and dimer of C1 conformers of molecule

are tabulated in Table 2 in comparison to the experimental values obtained from 2-ANA molecule crystal [19].

To determine the most stable energy conformation of the 2-ANA molecule, a conformation analysis was performed between pyridine ring and COOH group system on C1–C2–C7–O8 and O9–C7–O8–C12 atoms. To explain conformational features of 2-ANA, the selected degree of torsional freedom, $T(C1-C2-C7-O8)$ and $T(O9-C7-O8-C12)$, was varied from 0° to 360° in very 10° and the molecular energy profile was obtained with the B3LYP/6-311++G(d,p) method. Namely, potential energy curve was computed by means of scanning COOH group made over the ring group spin and H12 atom rotated around O8 atom. All the scans show that C1 form of the 2-ANA had a planar C_s point group symmetry, shown evident H12 position and carboxylic acid position.

The conformational energy profile shows two maxima near 90° and 270° both $T(C1-C2-C7-O8)$ and $T(O9-C7-O8-H12)$ torsion angles, respectively. The aromatic rings are nearly perpendicular at these values of selected torsion angle. It is clear from Fig. 3, there are three local minima observed at 0°, 180° and 360° for both $T(C1-C2-C7-O8)$ and $T(O9-C7-O8-H12)$ torsion angles, respectively. Therefore, the most stable conformer is for 0° torsion angle $T(C1-C2-C7-O8)$ and for 180° torsion angle $T(O9-C7-O8-H12)$. The DFT optimized geometry of the crystal structure is coplanar at these values of selected torsion angle.

The theoretical values showed that most of the optimized bond lengths and angles have some discrepancies from experimental values. These discrepancies may result from that the theoretical

Table 1
Calculated energies and energy difference for four conformers of 2-ANA by DFT/B3LYP 6-311++G(d,p) method.

Conformers	Energy		Energy differences ^a		Dipol moment (Debye)
	(Hartree)	(kcal mol ⁻¹)	(Hartree)	(kcal mol ⁻¹)	
C1	–492.3817	–308974.2205	0.0000	0.0000	1.2237
C2	–492.3775	–308971.5325	0.0043	2.6880	1.5125
C3	–492.3698	–308966.7355	0.0119	7.4850	3.4345
C4	–492.3513	–308955.1023	0.0305	19.1182	4.2514

^a Energies of the other three conformers relative to the most stable C1 conformer.

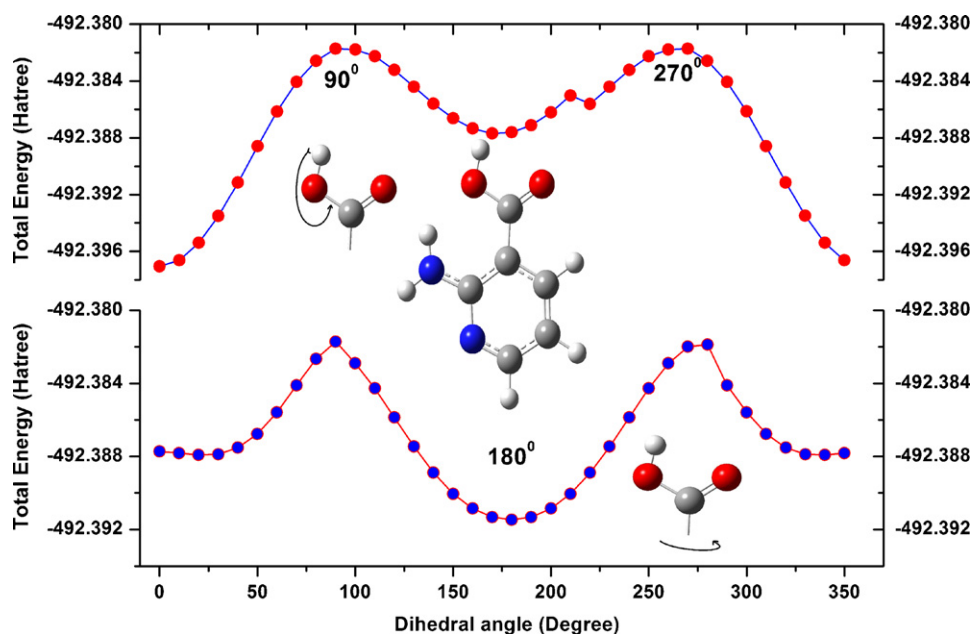


Fig. 3. PES scan for the selected degree. (a) $T(\text{C1—C2—C7—O8})$ and (b) $T(\text{O9—C7—O8—H12})$ torsional freedom.

calculations belong to isolated molecule in gaseous phase and the experimental results belong to molecule in solid state. Hence, taking into account that the molecular geometry in the vapour phase may be different from in the solid phase, owing to extended hydrogen bonding and stacking interactions there is reasonable agreement between the calculated and experimental geometric parameters. The CN bond distance, C1–N10 and C1–N14 evaluated in the present work with DFT(B3LYP) method are 1.350 Å and 1.351 Å, respectively. These results are in excellent agreement with those of previously reported experimental results using X-ray diffraction [19]. The calculated bond distance values of C7=O9 is 1.358 Å and C7–O8 is 1.220 Å. The corresponding bond lengths are 1.266 Å (C=O) and 1.234 Å (C–O) with X-ray [19]. The similar correlation was found for similar molecules in the literature [27–30].

Literature survey reveals that to the best of our knowledge, no experimental geometric dimer structure of 2-ANA is published in the literature yet. Therefore, we could not compare the calculation results for 2-ANA dimer structure with the experimental data. However, the intermolecular hydrogen bonds are almost linear (the O–H...O angle equals 177.2°) and their length is 1.723 Å [31], and in COOH group for 5-fluoro-salicylic acid, the angle and length are 179.6° and 1.676 Å respectively [30]. In this study, we calculated these angles and lengths 180° and 1.778 Å and 1.783 Å, showed a good coherent with literatures.

4.3. Vibrational spectra

The present molecule consists of 16 atoms, so it has 42 normal vibrational modes. On the basis of C_s symmetry the 42 fundamental vibrations of title molecule can be distributed as $29A' + 13A''$. The vibrations of the A' species are in plane and those of the A'' species are out of plane. The symmetry species of all the vibrations, a detailed description of the normal modes based on the total energy distribution (TED), experimental wavenumbers with the calculated for monomer and dimer C1 conformer of studied molecule are given in Table 3. Modes are numbered from biggest to smallest frequency within each fundamental wavenumbers, ν .

In order to acquire the spectroscopic signature of 2-ANA molecule, we performed a frequency calculation analysis. The

calculations were made for free molecule in vacuum, while experiments were performed for solid sample, so there are disagreements between calculated and observed vibrational wavenumbers, and some frequencies are calculated, however these frequencies are not observed in the FT-IR spectrum. To compare, we use the experimental (FT-IR and FT-Raman) data of 2-ANA, studied by Świsłocka et al. [15].

Fig. 4 presents the experimental and calculated infrared spectra. The calculated IR spectrum is shown in figure for comparative purposes, where the calculated intensity is plotted against the harmonic vibrational frequencies. The vibrational spectrum was obtained by molecular orbital calculation using Gaussian 03 [24] program. Vibrational modes of 2-ANA were researched by harmonic frequency calculations performed at the corresponding energy optimized geometries. The assignment of the vibrational absorptions was made by the comparison with the related molecule and also with the results obtained from the theoretical calculations. As seen in Table 3, there is great mixing of the ring vibrational modes and also between the ring and substituent modes. The descriptions of the modes are very complex because of the low symmetry of the studied molecule. Especially, in plane, out of plane and torsion modes are the most difficult to assign due to mixing with the ring modes and also with the substituent modes. But there are some strong frequencies useful to characterize in the IR spectrum.

The correlation graphic described harmony between the calculated and experimental wavenumbers (Fig. 5). The relations between the calculated and experimental wavenumbers are linear and described by the following equation:

$$\nu_{\text{cal}} = 0.9303 \nu_{\text{exp}} + 67.3367$$

We calculated correlation coefficients (R^2) value ($R^2 = 0.9956$) between the calculated and experimental wavenumbers. As a result, the performance of the B3LYP method with respect to the prediction of the wavenumbers within the molecule was quite close.

4.3.1. O–H vibrations

The O–H vibrations are extremely sensitive to formation of hydrogen bonding. The O–H stretching band is characterized by very broadband appearing near about $3400\text{--}3600\text{ cm}^{-1}$ [32,33].

Table 2
Bond lengths (Å) and bond angles (°) experimental and optimized of 2-ANA for C1 conformer.

Parameters	X-ray ^a	B3LYP/6-311++G(d,p)	
		Monomer	Dimer
Bond lengths (Å)			
C1–C2	1.423 (2)	1.430	1.430
C1–N10	1.360 (2)	1.350	1.349
C1–N14	1.322 (2)	1.351	1.351
C2–C3	1.374 (3)	1.400	1.400
C2–C7	1.514 (2)	1.466	1.466
C3–C4	1.398 (3)	1.385	1.385
C3–H11	0.970 (2)	1.082	1.082
C4–C5	1.355 (3)	1.398	1.398
C4–H6	0.910 (2)	1.082	1.082
C5–N10	1.348 (2)	1.326	1.326
C5–H13	1.020 (2)	1.087	1.087
C7–O8	1.234 (2)	1.220	1.220
C7–O9	1.266 (2)	1.358	1.358
O8–H12	–	0.968	0.968
N14–H15	0.940 (3)	1.010	1.010
N14–H16	0.880 (2)	1.007	1.006
Bond angles (°)			
C2–C1–N10	118.2	121.6	121.6
C2–C1–N14	124.4	122.5	122.5
N10–C1–N14	117.4	115.9	115.9
C1–C2–C3	118.2	117.7	117.7
C1–C2–C7	122.0	120.9	120.9
C3–C2–C7	119.8	121.5	121.4
C2–C3–C4	121.7	120.3	120.3
C2–C3–H11	119.6	118.8	118.8
C4–C3–H11	–	120.9	120.9
C3–C4–C5	118.2	117.4	117.4
C3–C4–H6	–	121.7	121.7
C5–C4–H6	119.1	120.8	120.8
C4–C5–N10	121.2	124.4	124.4
C4–C5–H13	–	120.1	120.1
N10–C5–H13	115.5	115.5	115.5
C2–C7–O8	117.5	113.6	113.6
C2–C7–O9	116.9	125.7	125.7
O8–C7–O9	125.6	120.7	120.7
C7–O8–H12	–	106.5	106.5
C1–N10–C5	122.5	118.6	118.6
C1–N14–H15	113.3	120.0	120.0
C1–N14–H16	122.4	117.7	117.7
H15–N14–H16	124.3	122.3	122.3
Selected dihedral angles (°)			
C2–C1–N14–H15	–	0	0
C2–C1–N14–H16	–	180	180
C2–C7–O8–H12	–	180	180
O9–C7–O8–H12	–	0	0
Intermolecular H bond lengths and angles			
O(9)···H(23)	–	–	1.778
H(12)···O(17)	–	–	1.783
O(9)···H(23)	–	–	180.0
H(12)···O(17)	–	–	180.0

^a The X-ray data from ref. [19].

Koczoń et al. [2] assigned OH stretching vibration at 3447 cm^{-1} IR and calculated at 3651 cm^{-1} for nicotinic acid. In previous study [34], this band was recorded at 3684 cm^{-1} (FT-IR) and predicted at 3610 cm^{-1} which agreed with recorded FT-IR data. The hydrogen bonding in the condensed phase with the other acid molecules makes vibrational spectra more complicated. Therefore, we could not observe the strong and sharp bands of the O–H vibration in the IR spectra. However, this band is calculated at 3616 cm^{-1} .

It can be observed that there is a frequency downshift of O–H stretching vibration in dimer due to the presence of intermolecular interaction. The occurrence of dimeric conventions is due to hydrogen bonds which act as the bridging mode. In our previous work [35], the lower stretching frequency observed in 4-butyl benzoic acid compared with the free O–H group stretching signifies that there is a possibility of intermolecular hydrogen bonding in 4-butyl benzoic acid, between the hydroxyl group of one molecule

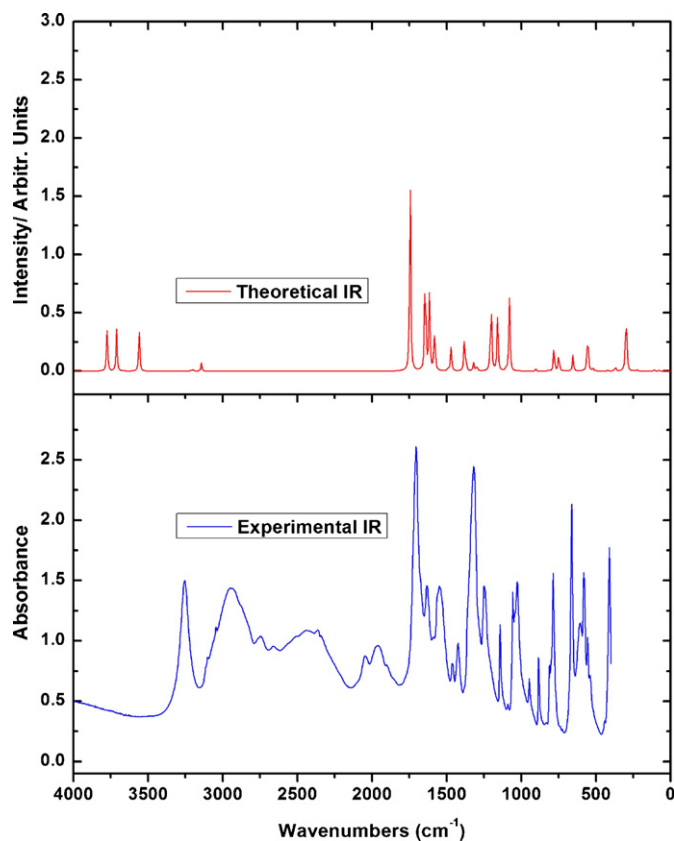


Fig. 4. Theoretical and experimental FT-IR spectrum of 2-ANA.

and carbonyl group of another molecule. Also this study showed that there was a frequency downshift of O–H stretching vibration in dimer due to the presence of intermolecular interaction. One can see O–H stretching vibration calculated at 3616 cm^{-1} for monomeric structure and at $3008\text{--}3090\text{ cm}^{-1}$ for dimeric structure which agreement with above interpretation. This mode is pure stretching mode as it is evident from TED column 100%.

The O–H in plane bending vibration occurs in the general of $1440\text{--}1395\text{ cm}^{-1}$. The O–H out of plane bending vibration occurs in $960\text{--}875\text{ cm}^{-1}$ [36]. In prior investigation, for 2-chloronicotinic acid, O–H in plane bending and out of plane bending vibrations were assigned to 1406 and $834(828)\text{ cm}^{-1}$, respectively. Theoretically computed values (1393 and 830 cm^{-1}) are in very good agreement with experimental results [17,34]. The O–H in-plane

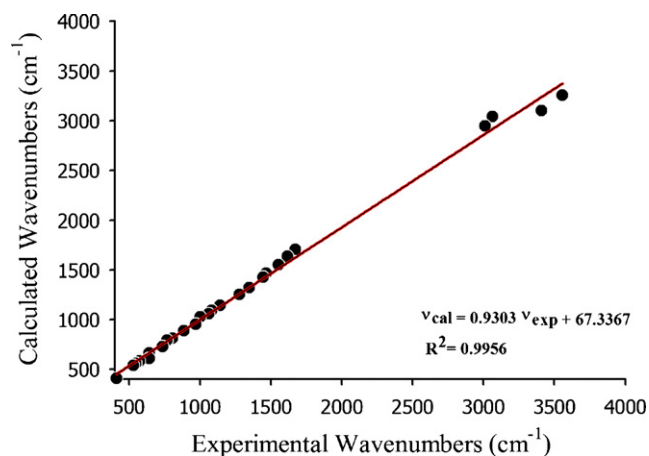


Fig. 5. Correlation graphic of calculated and experimental frequencies of 2-ANA.

Table 3Comparison of the calculated harmonic frequencies and experimental (FT-IR and FT-Raman) wavenumbers (cm^{-1}) using by B3LYP method and 6-311++G(d,p) basis set for the C1 conformer of 2-ANA.

Modes no.	Sym. species	Theoretical monomer		Theoretical dimer		Experimental		This study FT-IR	TED ^c ($\geq 10\%$)
		Unscaled freq.	Scaled freq. ^a	Unscaled freq.	Scaled freq. ^a	FT-IR ^b	FT-Raman ^b		
ν_1	A'	3775	3616	3225, 3140	3090,3008				νOH (100)
ν_2	A'	3712	3556	3717, 3716	3561,3560	3257m		3256s	νNH_2 asym. (100)
ν_3	A'	3560	3411	3570, 3570	3420,3420	3099sh	3107m	3102sh	νNH_2 sym. (100)
ν_4	A'	3212	3078	3212, 3212	3077,3077				νCH sym. (99)
ν_5	A'	3197	3063	3197, 3197	3063,3063	3045sh	3046w	3044sh	νCH asym. (98)
ν_6	A'	3144	3012	3144, 3144	3012,3012	2950–2658m		2946m	νCH (98)
ν_7	A'	1745	1672	1703, 1668	1640,1631	1703vs	1682vw	1706s	$\nu\text{C}=\text{O}$ (82)
ν_8	A'	1645	1617	1641, 1640	1613,1611	1636m	1632w	1634m	ρNH_2 (26) + νCC (25) + $\nu\text{CN}10$ (19)
ν_9	A'	1617	1589	1616, 1614	1589,1587	1603m			ρNH_2 (51) + νCC (27)
ν_{10}	A'	1581	1554	1581, 1579	1554,1552	1560s	1566m	1550s	νCC (36) + ρNH_2 (20) + νCN (14) + δCH (13)
ν_{11}	A'	1492	1466	1490, 1488	1465,1463	1463m		1464m	δCCH (44) + νCC (16) + νCN (12)
ν_{12}	A'	1470	1445	1470, 1453	1445,1429	1424m	1468w	1425m	$\nu\text{C}-\text{NH}_2$ (30) + νCC (20) + δCH (20) + ρNH_2 (14)
ν_{13}	A'	1381	1358	1495, 1452	1470,1427	1384m	1370w		νCO (24) + δCOH (24) + νCC (15) + νCN (10)
ν_{14}	A'	1370	1347	1377, 1375	1354,1352	1321s	1318vs	1320vs	$\nu\text{CN}10$ (26) + δCNH (23) + νCNH_2 (13) + δCOH (12)
ν_{15}	A'	1321	1298	1314,1314	1292, 1292				τNH_2 { δCNH } (27) + δCCH (20) + νCN (18) + νCC (16)
ν_{16}	A'	1299	1277	1272, 1271	1250, 1249	1251m	1250m	1250m	νCC (32) + δCCH (19) + νCN (17)
ν_{17}	A'	1203	1183	1350, 1344	1327, 1321				δCOH (40) + νCC (28) + δCCH (15)
ν_{18}	A'	1161	1141	1173, 1170	1153, 1150	1143m	1144w	1141m	δCCH (54) + νCC (19) + δCOH (10) + τNH_2 (10)
ν_{19}	A'	1102	1083	1099, 1099	1081, 1081	1089w	1082vw	1092vw	νCC (46) + τNH_2 { δCNH } (17) + δCCH (15) Ring Breathing
ν_{20}	A'	1081	1063	1125, 1123	1106, 1104	1058m	1058m	1058m	$\nu\text{C}-\text{O}$ (43) + νCC (15) + δCCH (15) Ring Deformation
ν_{21}	A'	1021	1003	1020, 1020	1002, 1002	1029m	1034m	1025m	νCN (36) + τNH_2 { δCNH } (34) + νCC (14) + δCCH (15) Ring Breathing
ν_{22}	A''	987	971	990, 990	973, 973				γCH (88)
ν_{23}	A''	987	970	987, 987	970, 970	948m	960w	949m	γCH (90)
ν_{24}	A'	903	888	907, 907	891, 892	885m	889m	887m	$\nu\text{C}-\text{NH}_2$ (22) + δCCC (38) + δCCN (25) Ring Breathing, David's star
ν_{25}	A''	820	806	824, 822	810, 809	831w/812m	808vs	812sh	τCCCO (40) + γCH (18) + τCCCN (24)
ν_{26}	A''	783	769	782, 782	768, 768	790m		789s	γCH (66) + τCCCN (20)
ν_{27}	A''	751	738	748, 746	736, 734	727w	729vw	725vw	τCCCN (38) + τCCCO (30) + τCCOH (18)
ν_{28}	A'	749	736	793, 777	780, 764				νCC (46) + δCOO (17) + νCO (10)
ν_{29}	A'	656	644	679, 674	668, 662	664s	663s	660vs	δOCO (33) + δCCO (17) + δCCN (13) + δCCC (13)
ν_{30}	A''	652	641	650, 649	639, 638	617m		608w	τNH_2 (95)
ν_{31}	A'	584	574	586, 586	576, 576	583m	581s	580m	δCCN (34) + δCCC (28) + δNCN (10)
ν_{32}	A''	556	547	960, 866	944, 851	557m	552vw	555m	γOH (87)
ν_{33}	A''	539	530	540, 539	531, 530			539sh	τCCCN (31) + τCCCH (22) + τCCCC (18) + τCCNH (11)
ν_{34}	A'	518	509	551, 531	542, 522				δCCO (39) + τNH_2 (22) + δCCC (14) + νCC (10)
ν_{35}	A''	425	418	433, 433	426, 426	442w	442vw		τCCCC (29) + τCCCN (28) + τCCCO (15) + τCCOH (12)
ν_{36}	A'	420	413	443, 440	436, 432	411m	409w	408s	δCCN (39) + δCCO (17) + νCC (19)
ν_{37}	A'	371	364	387, 380	381, 374				νCC (24) + δNCN (28) { τNH_2 } + δCCC (17) + δCCO (15)
ν_{38}	A''	300	294	292, 288	287, 284				ωNH_2 (97)
ν_{39}	A'	249	244	296, 292	290, 287				τCOOH (96) { δCCC (68) + δCCO (28)}
ν_{40}	A''	226	222	237, 232	233, 228				τCCCN (23) + τCCCC (22) + τCNCN (21) + τCCCO (17)
ν_{41}	A''	110	108	119, 111	117, 110				τCCCN (63) + τCCCC (13) + τCCCO (11)
ν_{42}	A''	80	78	89, 77	87, 75				τCCCO (90) (τCOOH)

^a Wavenumbers in the ranges from 4000 to 1700 cm^{-1} and lower than 1700 cm^{-1} are scaled with 0.958 and 0.983 for B3LYP/6-311++G(d,p) basis set, respectively.^b Taken from ref. [15]; vs, very strong; s, strong; m, medium; w, weak; vw, very weak; sh, shoulder; sym., symmetric; asym., asymmetric.^c TED, total energy distribution; ν , stretching; γ , out-of plane bending; δ , in-plane-bending; τ , torsion; ρ , scissoring; t, twisting; r, rocking; ω , wagging.

and O–H out-of-plane bending banding of carboxylic acids appear between 1179 and 549 cm^{-1} (FT-IR) [35]. In this present work the O–H in-plane bending vibration calculated at 1183 and 1358 cm^{-1} . The O–H out-of-plane vibration gives a broad band at 555(m) cm^{-1} . The theoretically computed values at 547 cm^{-1} show moderate agreement with recorded spectrum. In dimer conformations, the O–H in plane bending and out of plane bending vibrations values are increasing, because of the hydrogen bonding effect through the carboxyl groups (vide Table 3).

4.3.2. N–H vibrations

The amino group gives rise to internal modes of vibrations, for example; the asymmetric stretching, symmetric stretching, scissoring, rocking, wagging and twisting. NH_2 , CH_2 and CH_3 asymmetric stretching modes have higher magnitude than the symmetric stretching [33]. The asymmetric NH_2 stretching vibration appears from 3420 to 3500 cm^{-1} and the symmetric NH_2 stretching is observed in the range of 3340–3420 cm^{-1} [37]. The corresponding symmetric mode occurs in the experiment at 3393 cm^{-1} and asymmetric mode at 3507 cm^{-1} for 2-aminoterephthalic acid and also N–H asymmetric and symmetric stretching vibrations were assigned at 3526 and 3432 cm^{-1} , respectively in NH_2 group [38]. These vibrations were calculated at 3555 and 3436 cm^{-1} by using same method for nicotinamide N-oxide in previous work [39]. The 2-ANA molecule has only one NH_2 group hence, expects one symmetric and one asymmetric N–H stretching vibrations in NH_2 group. The vibrational frequencies described by modes 2 and 3 assigned to the NH_2 asymmetric and symmetric stretching modes, calculated at 3556 and 3411 cm^{-1} , respectively. In this study, asymmetric and symmetric NH_2 mode is observed in FT-IR (3256(s) and 3102(sh) cm^{-1}). As expected these two modes are pure stretching modes as it is evident from TED column, they are almost contributing 100%.

NH_2 scissoring deformation appears in the 1638–1575 cm^{-1} region with strong to very strong IR intensity [33]. As recorded in previous study, as a strong band at 1591 cm^{-1} is identified with NH_2 scissoring which also contributes with C–C stretching mode. This deviates negatively by ca. 15 cm^{-1} from expected characteristic value [38]. The NH_2 scissoring mode for nicotinamide N-oxide is observed at 1609 cm^{-1} in the FT-Raman and calculated 1596 cm^{-1} using B3LYP method [39]. It is seen in Table 3, the present calculations give NH_2 scissoring mode at 1617 cm^{-1} , shows very good coherent with experimental value (1634 cm^{-1}). The rocking mode of the amino group appears in the range of 1000–1100 cm^{-1} with variable IR intensity. According to the TED, we calculated this band at 1298 cm^{-1} , however we did not observe this mode in FT-IR.

In prior work [38], the wagging (torsion) and rocking fundamentals are assigned to the calculated bands at 227 and 1036 cm^{-1} for 2-aminoterephthalic acid. The NH_2 twisting vibration calculated at 599 cm^{-1} is missing in FT-IR spectrum [38]. For 2-ANA, we predicted the wagging (out-of-plane bending) and rocking fundamentals are assigned to the calculated bands at 294 and 1141 cm^{-1} missing in FT-IR spectrum, respectively. The NH_2 twisting mode is calculated at 641 cm^{-1} and at 638, 639 cm^{-1} for monomer and dimer, observed 608 cm^{-1} in FT-IR. This NH_2 twisting vibration is calculated at low wavenumbers with maximum TED contribution (95%). Also this mode was observed at 617 cm^{-1} in FT-IR spectrum by Świsłocka et al. [15]. The observed medium band at 1025 cm^{-1} in IR attributed to the appreciable contribution from the CNH angle bending suggesting its origin due to the rocking mode. It is a strongly mixed mode containing contribution from the CN stretching and the rocking modes.

The C– NH_2 stretching mode was obtained at 1233 and 1453 cm^{-1} in the experimental FT-IR spectrum, coupled with the ring modes [38]. The C– NH_2 stretching mode were observed at 938 cm^{-1} in FT-IR (936 cm^{-1} in FT-Raman), calculated 941 and

939 cm^{-1} for trans and cis form of the nicotinamide N-oxide respectively [39]. For the investigated molecule, we predicted at 1445 and 888 cm^{-1} , show in good agreement with the experimental values (1425(m) and 887(m)). It is worth mentioned that C– NH_2 stretching modes values in dimer conformation are decreasing (except mode ν_{29}), this may can be due to the hydrogen bonding effect through the carboxyl groups.

4.3.3. C–H vibrations

For all the aromatic compounds the carbon–hydrogen stretching vibrations are observed in the region of 3000–3100 cm^{-1} range which is the characteristic region for the ready identification of C–H stretching vibrations and these vibrations are not found to be affected due to the nature and position of the substituent [32,40,41]. Accordingly, in this work, the three adjacent hydrogen atoms left around the pyridine ring, the 2-ANA give rise three C–H stretching modes (ν_4 – ν_6), are predicted in the range of 3012–3078 cm^{-1} . They are very pure modes since their TED contribution are 98–100%. These modes were recorded in this region which correspond to 2946(m) and 3044(sh) cm^{-1} and show excellent agreement with predicted values.

The C–H in-plane bending frequencies appear in the range of 1000–1300 cm^{-1} and C–H out-of-plane bending vibration in the range of 750–1000 cm^{-1} in the aromatic compounds [32,41,42]. The C–H in plane bending and C–H out-of-plane bending vibrations are calculated at 1003–1466 cm^{-1} and 769–971 cm^{-1} , respectively. Both the in-plane and out-of-plane bending vibrations are described as mixed modes. Namely, C–H bending modes generally are contaminated by other vibrations. In generally the aromatic C–H vibrations (stretching, in-plane and out-of-plane bending) calculated theoretically are in good agreement with experimentally accepted values. In this study, the C–H in plane bending vibrations were recorded at 1464 and 1141 cm^{-1} and the C–H out-of-plane bending vibrations were assigned at 949 and 789 cm^{-1} which agree with calculated data. According to TED contribution in-plane and out-of-plane modes indicate that out-of plane modes are also highly pure modes like the in-plane bending fundamentals. Summary, all results of C–H modes are very good coherent with our earlier report [27,30,38,39] and also lie within the characteristic region.

4.3.4. C–O and C=O vibrations

The band observed in the 1700–1800 cm^{-1} region is usually the most characteristic feature of carboxylic group. This band is due to the C=O stretching vibration. Also Koczoń et al. [2] observed the range of 1800–1500 cm^{-1} , the CC, C=O and COOH group stretching vibrations. The C=O stretching vibration of the 2-ANA was observed at 1706(s) cm^{-1} in FT-IR spectrum and predicted at 1672 cm^{-1} in very good coherent with empirical values. Also this mode was observed at 1703 and 1682 cm^{-1} in FT-IR and FT-Raman spectrum by Świsłocka et al. [15].

The C–O stretching vibration is assigned at 1058 cm^{-1} in FT-IR and calculated at 1063 cm^{-1} which has the TED value of 43%. The very strong band in Infrared spectrum is assigned to O=C=O bending vibration (660 cm^{-1}) whereas the scaled B3LYP predicted value at 662 cm^{-1} shows a small deviation of about ca. 2 cm^{-1} for dimer structure. The C–O and C=O vibrations also show fairly good coherent in literature [27,30,39,43–45].

4.3.5. CN vibrations

The identification of C–N vibrations is a very difficult task, since the mixing of several bands is possible in this region. The ring C–N stretching vibration occurs in the region of 1310–1290 cm^{-1} [46]. Kumar et al. [47] have calculated the frequency for the CN stretching mode lies in the region of 1350–1370 cm^{-1} for both nicotinic acid and its N-oxide with strong IR intensity. Also in our previous

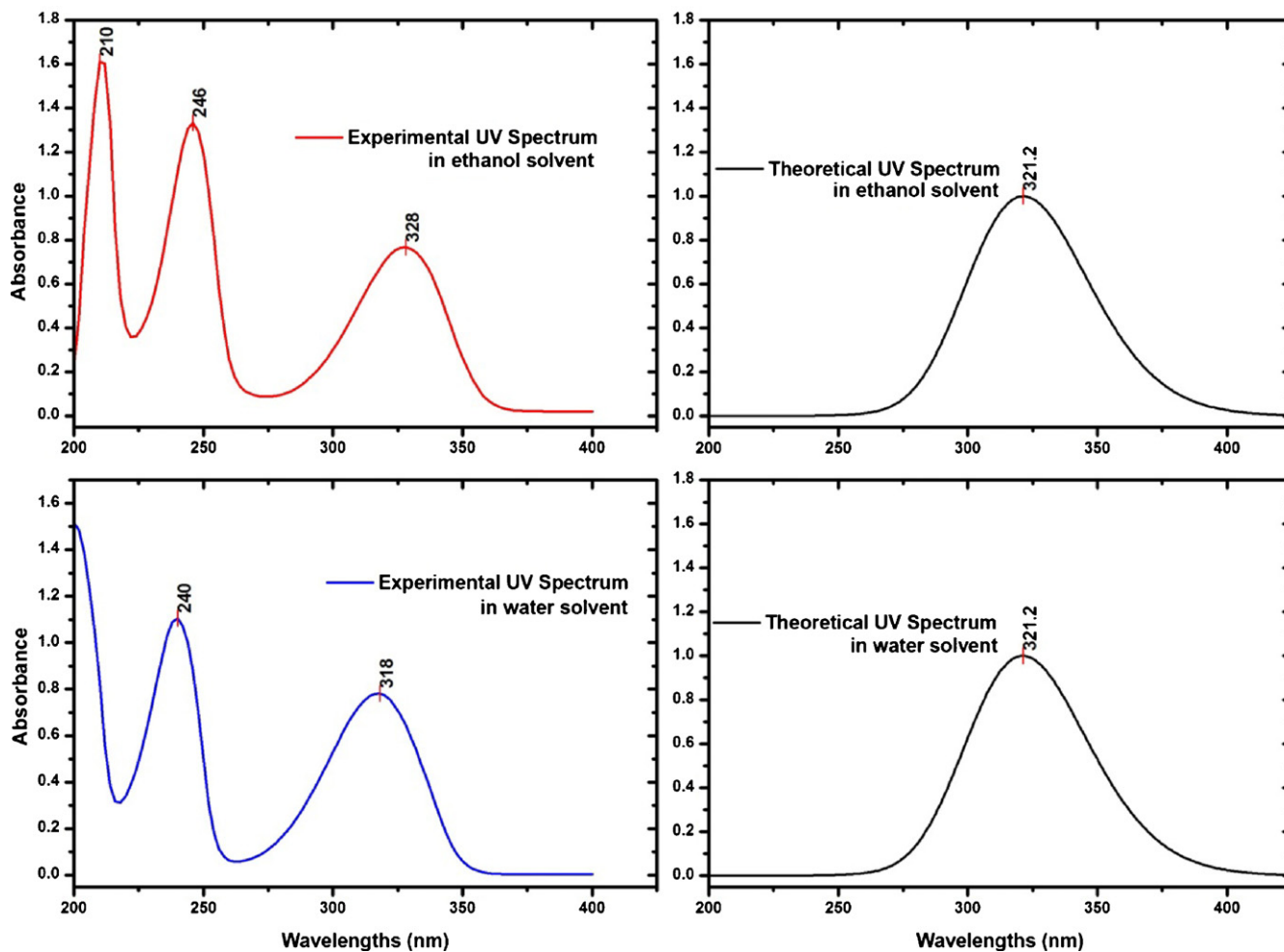


Fig. 6. Experimental and theoretical UV-vis spectrum of 2-ANA.

work [39], C=N and C–N stretching vibrations were observed at $742\text{--}1568\text{ cm}^{-1}$ in FT-IR and at $936\text{--}1594\text{ cm}^{-1}$ in FT-Raman spectrum, respectively. This band was calculated at $732\text{--}1561\text{ cm}^{-1}$ by using B3LYP method is in very good agreement with experimental values. The highest contribute assigned for this vibration at about 1231 cm^{-1} . In the present work, the frequencies computed by B3LYP method for our title molecule at 1347 and 1003 cm^{-1} for CN modes. The very strong and medium peaks at $1320(\text{vs})$ and $1025(\text{m})$ in FT-IR spectrum are assigned CN modes. According to TED, the peaks at 1445 and 888 cm^{-1} (1425 and 887 cm^{-1} in FT-IR) have been assigned to C–NH₂ stretching vibrations. Because of the other CN modes were contaminated with the ring modes and contribution of the TED is lower than these modes, we have given no discussion about them. However these modes analyses were given in Table 3.

4.3.6. CC vibrations

The ring stretching vibrations are very much important in the spectrum of pyridine and its derivatives, and are highly characteristic of the aromatic ring itself. The aromatic ring carbon–carbon stretching vibrations occur in the region of $1430\text{--}1625\text{ cm}^{-1}$. In the present work the strong C=C aromatic stretch is observed in the region of $1250\text{--}1550\text{ cm}^{-1}$ in FT-IR spectrum. These modes are calculated in the range of $1277\text{--}1554\text{ cm}^{-1}$. In former works [20], the C–C aromatic stretch is observed in the region of $1449\text{--}1577\text{ cm}^{-1}$ in the FT-IR spectrum, at 1580 cm^{-1} in the FT-Raman spectrum (2-BrNA), $1419\text{--}1579\text{ cm}^{-1}$ in the FT-IR spectrum and at 1580 cm^{-1} in

the FT-Raman spectrum (6-BrNA) showing in agreement with the theoretical assignment given by DFT. Also we have assigned the C–C vibrations at 1581 cm^{-1} (FT-IR) and 1569 cm^{-1} (FT-Raman) for 2-chloronicotinic acid [17] and at 1582 cm^{-1} (FT-IR), 1584 cm^{-1} (FT-Raman) for 6-chloronicotinic acid [16]. These modes, known as semicircle stretching modes calculated at $1437\text{--}1619\text{ cm}^{-1}$ (extensive region) is in excellent agreement with experimental values for nicotinamide N-oxide [39]. And also good correlation was found for pyridine [48], methyl pyridine [49].

4.3.7. Ring vibrations

The ring breathing vibrations are observed in the region of $1100\text{--}1000\text{ cm}^{-1}$. In this study, the ring deformation vibrations are assigned at medium $1058(\text{m})\text{ cm}^{-1}$ whereas the breathing vibrations are assigned at 1092 and 1025 cm^{-1} . The ring deformation and breathing vibrations are calculated at 1063 , 1083 and 1003 cm^{-1} , respectively.

The medium band at 887 cm^{-1} is observed in the FT-IR spectrum whereas the scaled B3LYP predicted value is 888 cm^{-1} shows a small deviation of about ca. 1 cm^{-1} . As revealed by the calculated TED, these bands arise from the mode 23, which can be described as the “trigonal ring breathing” vibration or the “Star of David” vibration of the aromatic ring. Most of the torsional and out-of-plane vibrations are mixed vibrational modes as shown in the TED column in Table 3. The ring assignments proposed in this study are also in agreement with literature values [16–18,23,27–30].

Table 4

The bond distances (Å) and characteristic wavenumbers (cm^{-1}) related to C=O bond and O–H of 2-ANA.

Conformers	C=O bond $\delta_{\text{C}7=\text{O}9}$	Scaled freq. $\nu_{\text{C}7=\text{O}9}$	O–H bond $\delta_{\text{O}8-\text{H}12}$	Scaled freq. $\nu_{\text{O}8-\text{H}12}$
C1	1.220	1672	0.968	3616
C2	1.210	1700	0.968	3609
C3	1.213	1694	0.963	3672
C4	1.203	1722	0.957	3767

4.4. Bond distances and characteristic frequencies

The molecular structure of a most stable conformation has been completely examined not only by experimental methods but also by theoretical approaches. 2-ANA possess carboxylic acid established one of the most popular model systems for studying inter- and intra-molecular hydrogen bonds. In order to compare the strength of inter- and intra-molecular hydrogen bonding, some pieces of evidence from geometrical and vibrational motion behavior were chosen to identify the hydrogen bonding effect and the bond distances and the characteristic frequencies of atoms within various conformers or isomers is given in Table 4. According to the calculated values, the relationships between these distances and the strengths of hydrogen bonds are discussed here. We present flowing interpretation.

- The bond length of the carbonyl distance of C1 conformer is showed the longest one ($\delta_{\text{C}=\text{O}} = 1.220 \text{ \AA}$) the other conformers and it has the smallest frequencies ($\nu_{\text{C}=\text{O}}$) 1672 cm^{-1} . The previous work [34] we reported $D_{\text{C}12=\text{O}13}$ bond length as 1.206 \AA for the most stable conformer of the nicotinic acid N-oxide. Similar results were obtained for different molecules [16,18,29,34].
- The longest hydroxyl distances ($\delta_{\text{O}8-\text{H}12}$) 0.968 \AA for both C1 and C2 conformer of the title molecule and the smallest frequencies ($\nu_{\text{O}-\text{H}}$) 3616 and 3609 cm^{-1} , respectively, because of the O atom in $\text{O}=\text{COH}$ of the C1 and C2 conformer, which donates electron to form with H in hydroxyl only. Also parallel results were obtained for structurally similar molecules [16,29,34].
- If we consider dimer structure (inter-molecular hydrogen bonding) shown in Fig. 2 are tabulated in Table 3, we can see the inter-hydrogen bonding effect through the carboxyl groups is clearly for the mode numbered ν_1 , ν_7 , ν_{11} , ν_{14} and ν_{17} . These results are given for structurally similar molecules [16,18,27,29,34] and our invention is in fairly consistent with these works.

4.5. UV spectrum and electronic properties

Ultraviolet spectra analyses of 2-ANA have been investigated by theoretical calculation and experimental. The UV–vis spectra of 2-ANA is shown in Fig. 6, was measured in ethanol and water solution. Gauss-Sum 2.2 program [50] was used to calculate group contributions to the molecular orbitals (HOMO and LUMO) and prepare the density of states (DOS) spectra in Fig. 7. The DOS spectra were created by convoluting the molecular orbital information with GAUSSIAN curves of unit height. The calculations of the electronic structure of 2-ANA were optimized in singlet state. Then, the electronic transition was calculated by using TD-DFT/6-311++G(d,p) method. Calculations of the molecular orbital geometry show that the visible absorption maxima of this molecule correspond to the electron transition between frontier orbitals such as translation from HOMO to LUMO from HOMO – 1 to LUMO + 1. The HOMO energy characterizes the ability of electron giving, the LUMO characterizes the ability of electron accepting, and the gap between HOMO and LUMO characterizes the molecular chemical stability [51]. The energy gap between the HOMOs and LUMOs,

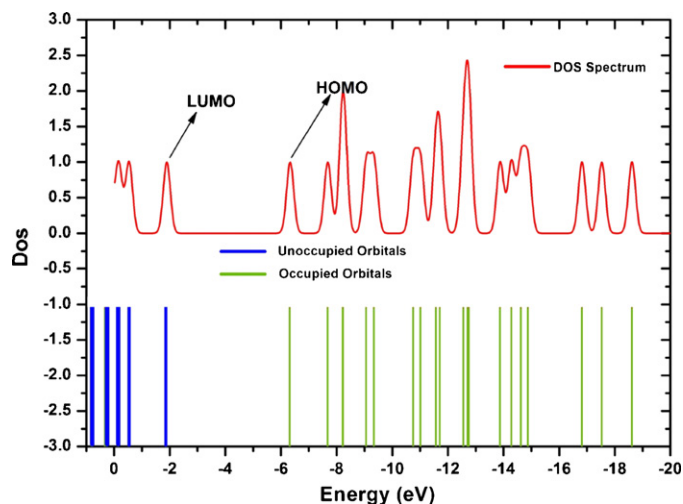


Fig. 7. Density of states (DOS) diagrams for 2-ANA.

is a critical parameter in determining molecular electrical transport properties because it is a measure of electron conductivity. To understand the bonding scheme of the 2-ANA, we depicted on the surfaces of the frontier orbitals; the second highest and highest occupied molecular orbitals HOMO and HOMO – 1 and the second highest and lowest unoccupied molecular orbitals LUMO and LUMO + 1, in Fig. 8 with the energy gap. Also the HOMO → LUMO transition for dimer of C1 structure of the title molecule showed Fig. 9. The HOMO shows a charge density localized mainly on the molecule overall and LUMO is characterized by a charge distribution on pyridine ring, carboxylic group and a little bit NH_2 group.

Absorption maxima (λ_{max} ; nm) for lower-lying singlet states of the molecule have been calculated by TD-DFT/B3LYP method for ethanol and water solvent. The calculated visible absorption maxima of λ which are functions of the electron availability has been reported in Table 5, are range of 322.13, 269.18 and 243.98 nm for in ethanol solvent, 320.46, 270.98 and 243.80 nm for in water solution. The spectrum shows three broad bands, a long wavelength band covering the 360–280 nm, a medium wave length one covering 280–240 nm region and a short wavelength one covering the 240–200 nm region. Each of these bands corresponds to a number of overlapping transitions. The experimental results are observed at 328, 246, 210 nm and 318, 240, 200 nm for in ethanol and water solution, respectively. We cannot say solvent effect according to experimental values as well as theoretical data. The absorption maxima values are fairly good agreement in theoretical values. The maximum absorption wavelength corresponds to the electronic transition from HOMO to LUMO 86%, from HOMO–1 to LUMO 96% and from HOMO–3 to LUMO 93% with contribution. The observed transition from HOMO to LUMO is $n-\pi^*$ one. Absorption spectrum of 2-ANA is quite different from the absorption spectra of its components. For example, λ_{max} is at 272 nm for nicotinic acid [52], 292 nm for 2-aminopyridine [53], and 288 for 4-aminobenzoic acid [54]. Nicotinamide absorption wavelength band observed at 262.0 and 214.0 nm [55]. However, for similar molecule 6-aminonicotinic acid, Dogra [14] observed absorption maxima of λ at 302 and 202 nm. These transitions are assigned n , π^* and π , π^* states in 6-ANA [14]. In this study, first transition is assigned n , π^* and the other two transitions are assigned π , π^* ones.

4.6. Thermodynamic properties

The values of some thermodynamic parameters (such as zero-point vibrational energy, thermal energy, specific heat capacity,

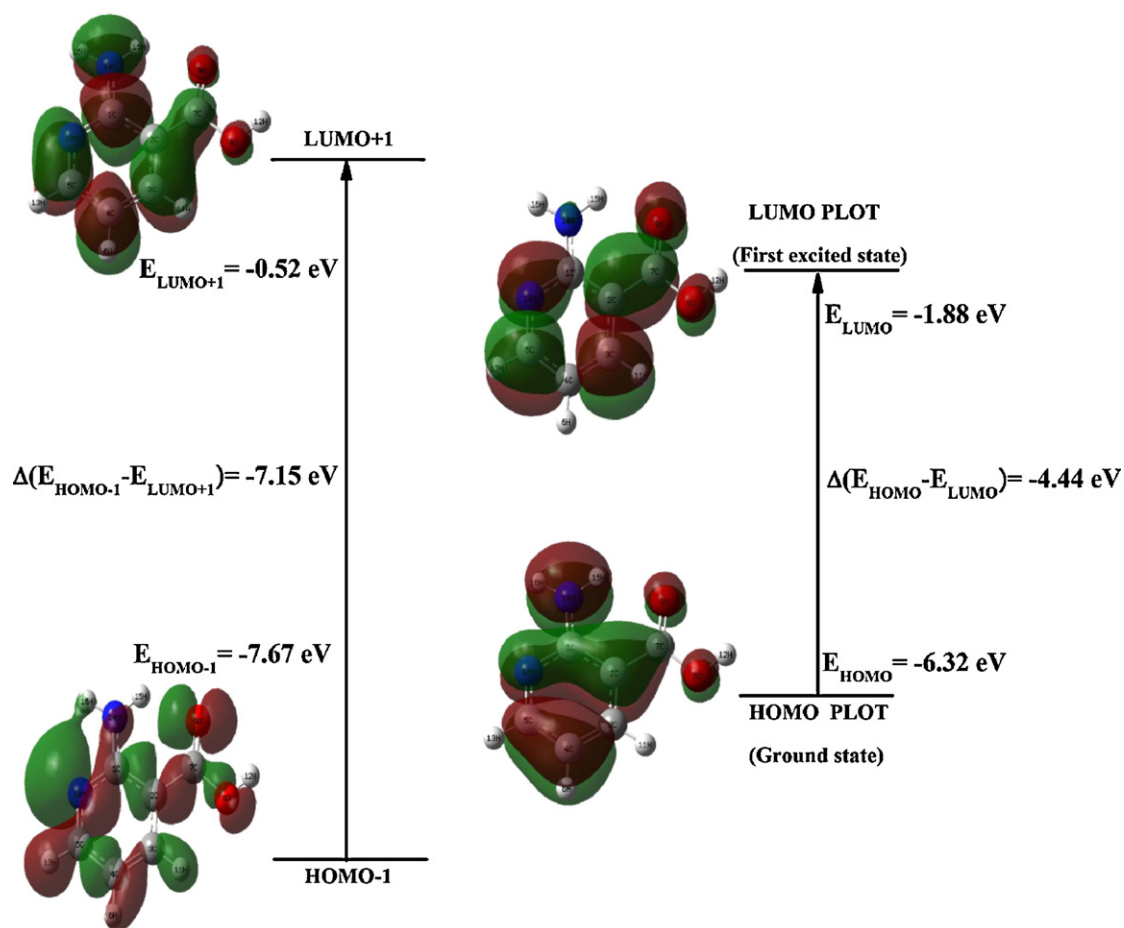


Fig. 8. The frontier molecular orbitals of 2-ANA by using B3LYP.

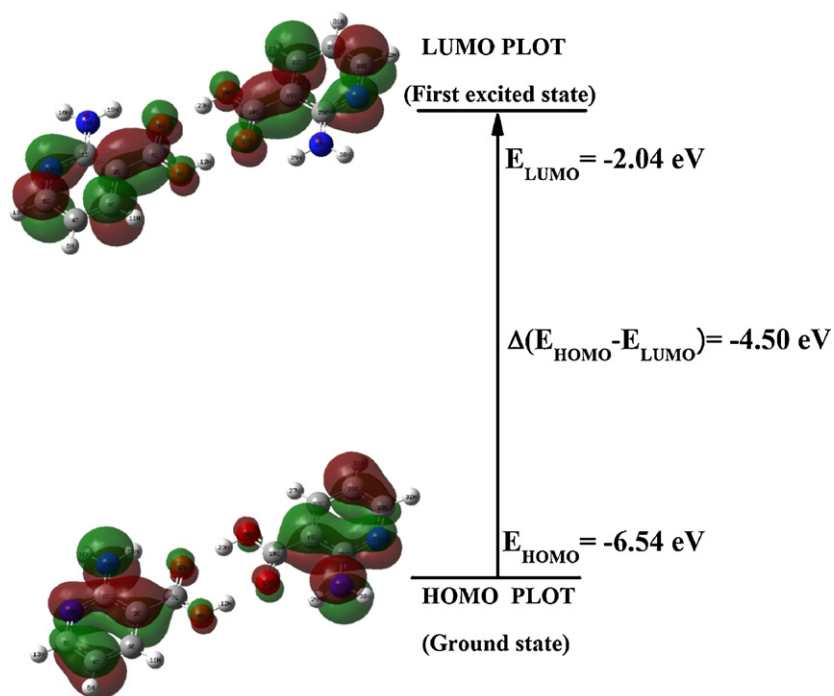


Fig. 9. The frontier molecular orbitals of dimer structure of 2-ANA for C1 conformer.

Table 5
Experimental and calculated wavelengths λ (nm), excitation energies (eV) and oscillator strengths (f) in ethanol and water solution.

Exp. (in ethanol)		Calculated			Assignments	Major contributors
λ (nm)	E (eV)	λ (nm)	E (eV)	f		
328	3.7849	322.13	3.8489	0.1578	$n \rightarrow \pi^*$	H \rightarrow L (86%)
246	5.0465	269.18	4.6060	0.0014	$\pi \rightarrow \pi^*$	H-1 \rightarrow L (96%)
210	5.9116	243.98	5.0817	0.0001	$\pi \rightarrow \pi^*$	H-3 \rightarrow L (93%)
Exp. (in water)		Calculated			Assignments	Major contributors
λ (nm)	E (eV)	λ (nm)	E (eV)	f		
318	3.9039	320.48	3.8686	0.1533	$n \rightarrow \pi^*$	H \rightarrow L (97%)
240	5.1726	270.98	4.5753	0.0014	$\pi \rightarrow \pi^*$	H-1 \rightarrow L (99%)
200	6.2072	243.80	5.0853	0.0001	$\pi \rightarrow \pi^*$	H-3 \rightarrow L (95%)

H, HOMO; L, LUMO.

Table 6
The calculated thermo dynamical parameters of 2-ANA at 298.15 K in ground state at the B3LYP/6-311++G(d,p) level.

Basic set	B3LYP/6-311++G(d,p)
SCF energy (a.u)	-492.38165079
Zero point vib. energy (kcal mol ⁻¹)	75.41645
Rotational constants (GHz)	2.360391,227990,80776
Specific heat, C_v (cal mol ⁻¹ K ⁻¹)	32.159
Entropy, S (cal mol ⁻¹ K ⁻¹)	89.689
Dipole moment (Debye)	1.1989

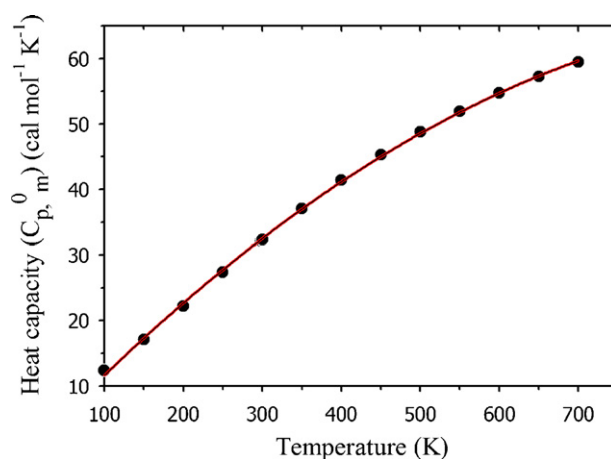
rotational constants, entropy, etc.) of 2-ANA at 298.15 K in ground state are listed in Table 6. The variation in Zero-Point Vibrational Energies (ZPVEs) seems to be significant. The value of ZPVE of 2-ANA are 75.41645 a.u. obtained at B3LYP/6-311++G(d,p).

On the basis of vibrational analysis, the statically thermodynamic functions: heat capacity ($C_{p,m}^0$), entropy (S_m^0), and enthalpy changes (ΔH_m^0) for the title molecule were obtained from the theoretical harmonic frequencies and listed in Table 7. From the Table 7, it can be observed that these thermodynamic functions are increasing with temperature ranging from 100 to 700 K due to the fact that the molecular vibrational intensities increase with temperature. The correlation equations between heat capacity, entropy, enthalpy changes and temperatures were fitted by quadratic formulas and the corresponding fitting factors (R^2) for these thermodynamic properties are 0.9995, 1.0000 and 0.9998, respectively. The corresponding fitting equations are as follows and the correlation graphics of those show in Figs. 10–12.

$$C_{p,m}^0 = -0.6586 + 0.1289T - 6.0945 \times 10^{-5}T^2 \quad (R^2 = 0.9995)$$

Table 7
Thermodynamic properties at different temperatures at the B3LYP/6-311++G(d,p) level for 2-ANA.

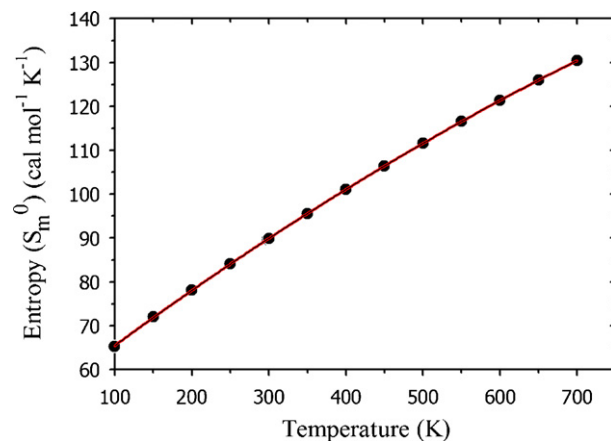
T (K)	$C_{p,m}^0$ (cal mol ⁻¹ K ⁻¹)	S_m^0 (cal mol ⁻¹ K ⁻¹)	ΔH_m^0 (kcal mol ⁻¹)
100	12.358	65.300	1.054
150	17.077	71.988	1.887
200	22.188	78.168	2.967
250	27.343	84.117	4.305
298.15	32.160	89.698	5.834
300	32.341	89.910	5.898
350	37.048	95.560	7.733
400	41.383	101.060	9.795
450	45.307	106.398	12.063
500	48.823	111.567	14.517
550	51.955	116.559	17.138
600	54.744	121.375	19.906
650	57.232	126.016	22.806
700	59.459	130.488	25.824

**Fig. 10.** Correlation graphic of heat capacity and temperature for 2-ANA.

$$S_m^0 = 52.2189 + 0.1361T - 3.4740 \times 10^{-5}T^2 \quad (R^2 = 1.0000)$$

$$H_m^0 = -0.4517 + 0.0093T + 4.0743 \times 10^{-5}T^2 \quad (R^2 = 0.9998)$$

All the thermodynamic data supply helpful information for the further study on the 2-ANA. They can be used to compute the other thermodynamic energies according to relationships of thermodynamic functions and estimate directions of chemical reactions according to the second law of thermodynamics

**Fig. 11.** Correlation graphic of entropy and temperature for 2-ANA.

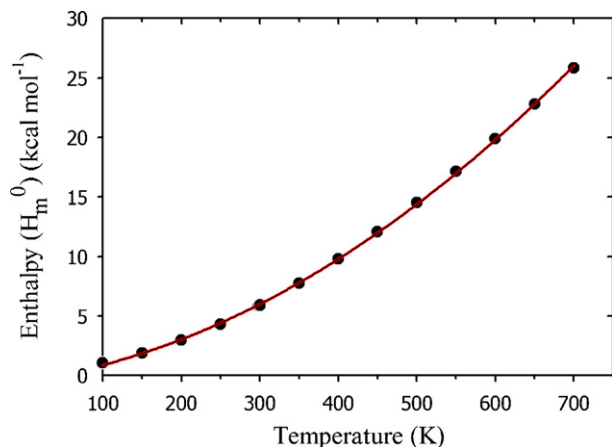


Fig. 12. Correlation graphic of enthalpy and temperature for 2-ANA.

in Thermochemical field. Notice: all thermodynamic calculations were done in gas phase and they could not be used in solution.

4.7. Molecular electrostatic potential

The MEP is a very useful feature to study reactivity given that an approaching electrophile will be attracted to negative regions (the electron distribution in where effect is dominant). In the majority of the MEPs, while the maximum negative region which preferred site for electrophilic attack indications as red colour, the maximum positive region which preferred site for nucleophilic attack symptoms as blue colour. The importance of MEP lies in the fact that it simultaneously displays molecular size, shape as well as positive, negative and neutral electrostatic potential regions in terms of colour grading and is very useful in research of molecular structure with its physiochemical property relationship. The resulting

Table 8

Mulliken charges of 2-ANA and nicotinic acid using B3LYP/6-311++G(d,p) basis set.

Atoms	2-Aminonicotinic acid	Nicotinic acid
C1	-0.754	-0.561
C2	0.972	0.447
C3	0.036	0.252
C4	-0.151	-0.137
C5	0.261	-0.315
H6	0.174	0.182
C7	-0.305	-0.304
O8	-0.196	-0.198
O9	-0.349	-0.291
N10	-0.126	-0.033
H11	0.229	0.238
H12	0.292	0.297
H13	0.190	0.188
N14/H14	-0.370	0.233
H15	0.318	-
H16	0.302	-

surface simultaneously displays molecular size and shape and electrostatic potential value. In the present study, 3D plots of molecular electrostatic potential (MEP) of 2-ANA has been drew in Fig. 13. The MEP is a plot of electrostatic potential mapped onto the constant electron density surface.

The different values of the electrostatic potential at the surface are represented by different colors. Potential increases in the order red < orange < yellow < green < blue. The color code of these maps is in the range between -0.05811 a.u. (deepest red) and 0.05811 a.u. (deepest blue) in compound, where blue shows the strongest attraction and red shows the strongest repulsion. Regions of negative $V(r)$ are usually associated with the lone pair of electronegative atoms. As can be seen from the MEP map of the title molecule, while regions having the negative potential are over the electronegative atoms (nitrogen atom in the ring and oxygen atom with collection COOH group), the regions having the positive potential are over the hydrogen atoms (especially H atom in where with collection COOH group). If compared, the negative potential values are -0.0354703 a.u. for oxygen atom (O atom for carboxylic acid) and -0.0353426 a.u. for N atom in the ring. However, the oxygen atoms have larger negative potential value than the nitrogen atom ones. A maximum positive region localized on the H atoms in the COOH group have value of $+0.0579637$ a.u. However, the H atoms at the NH_2 group and in the ring have smaller values than on the H atoms in the COOH group. According to these obtained results, we can say that the H atoms indicate the strongest attraction and O atoms indicate the strongest repulsion.

4.8. Mulliken atomic charges

Mulliken atomic charge calculation has a significant role in the application of quantum chemical calculation to molecular system because of atomic charges effect electronic structure, dipole moment, molecular polarizability and other properties of molecular systems. The calculated Mulliken charge values of 2-ANA and nicotinic acid are listed in Table 8. The charge distribution structure of 2-ANA is shown in Fig. 14. The results show that substitution of the aromatic ring by NH_2 group leads to a redistribution of electron density. For example, the charge of N10 and O9 atoms are negative in both molecule, however, because of added NH_2 group, the values of Mulliken atomic charge of N10 and O9 atoms are bigger than nicotinic acid. The oxygen and nitrogen atoms exhibit a negative charge, which are donor atoms. Moreover, O9 atom has bigger one more than N10 atoms. Hydrogen atom exhibits a positive charge, which is an acceptor atom, may suggest the presence of both intermolecular bondings with O9 atom which is a donor atom in the crystalline phase.

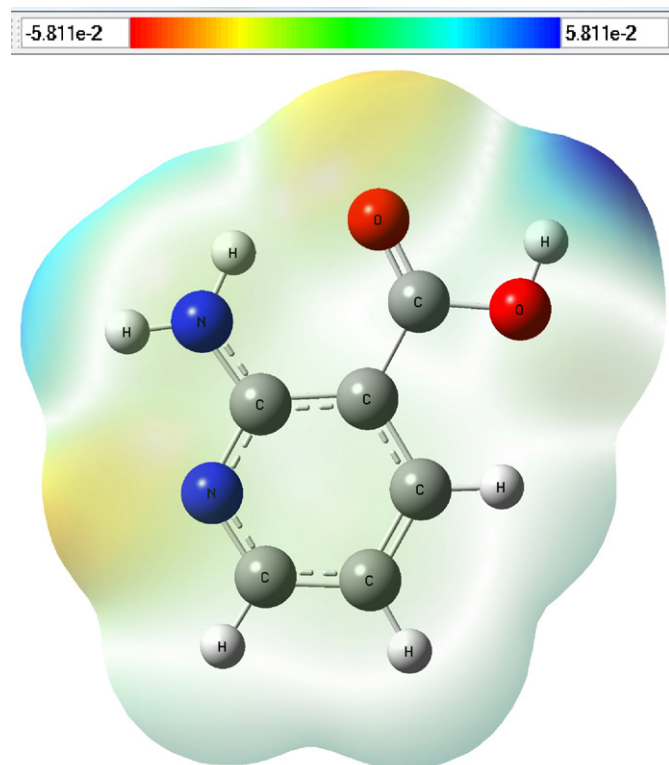


Fig. 13. Molecular electrostatic potential map (MEP) for 2-ANA.

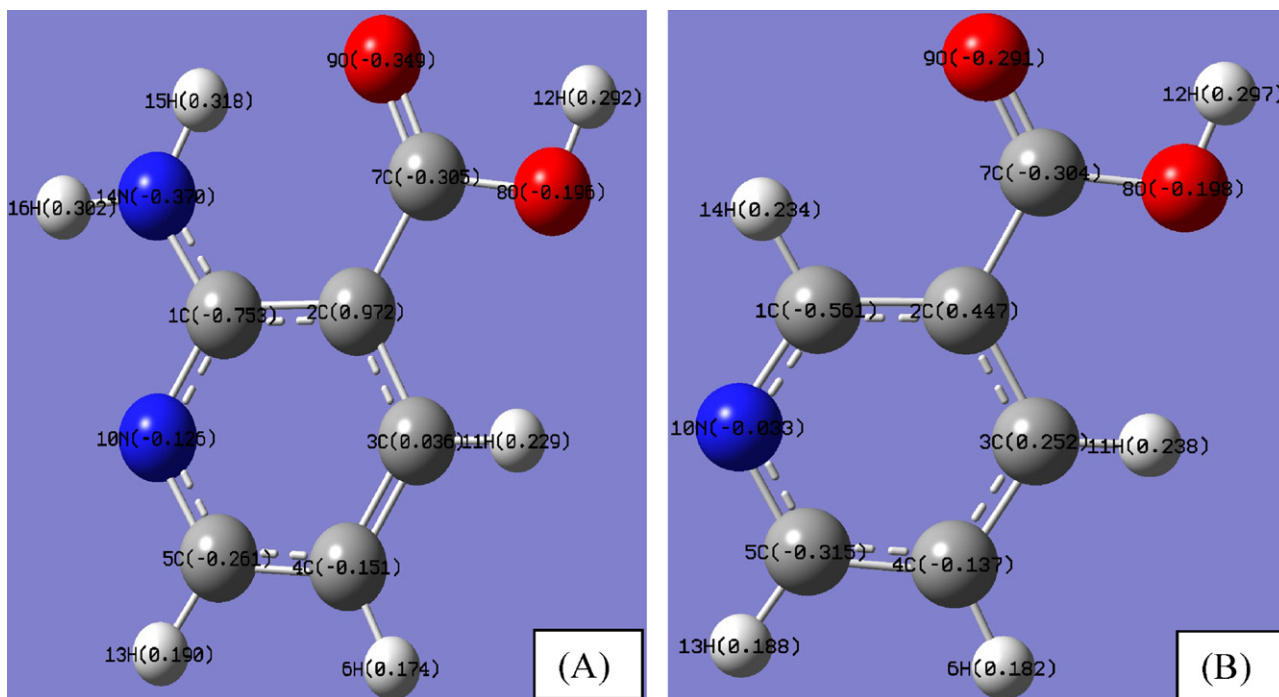


Fig. 14. The Mulliken charge distribution for 2-ANA.

5. Conclusions

In this study, the spectroscopic properties of the compound were examined by UV–vis and FT-IR techniques. Various quantum chemical calculations help us to identify the structural, conformational and symmetry properties of the molecule. The optimized geometric parameters (bond lengths and bond angles) were theoretically determined at B3LYP/6-311++G(d,p) level of theory and compared with X-ray results. The vibrational FT-IR spectra of 2-ANA was recorded. In order to identify its confidential conformational structure, potential energy curve was computed by means of scanning the selected degree of torsional freedom $T(C1-C2-C7-O8)$ and $T(O9-C7-O8-C12)$. A comparison of the result of experimental and theoretical study gave us a full description of the geometry and vibrational properties of title molecule. The existence of intermolecular interaction even in gaseous state has been confirmed by the construction of a dimer of compound and comparison of the theoretical and experimental high region frequencies. The results show that the hydrogen bonding interactions mainly affect the high frequency region while the skeletal vibration region keeps rather unchanged with the physical state of the samples. The electronic properties were also calculated and experimental electronic absorption spectra were recorded (200–400 nm) with help of UV–vis spectrometer. Also HOMO and LUMO energy of 2-ANA in the ground state have been calculated by using density functional theory for C1 and its dimer structure. The thermodynamic features of the title compound at different temperatures have been calculated. It is seen that the heat capacities, entropies and enthalpies increase with the increasing temperature owing to the intensities of the molecular vibrations increase with increasing temperature. The MEP map shows that the negative potential sites are on oxygen and nitrogen atoms as well as the positive potential sites are the hydrogen atoms in the amino group.

References

- [1] R. Chuck, Appl. Catal. A: Gen. 280 (2005) 75–82.
- [2] P. Koczoń, J. Cz. Dobrowolski, W. Lewandowski, A.P. Mazurek, J. Mol. Struct. 655 (2003) 89–95.
- [3] N.K. Singh, D.K. Singh, et al., Synth. React. Inorg. Met. Org. Chem. 32 (2002) 203–218.
- [4] C.L. Broadhurst, W.F. Schmidt, J.B. Reeves, M.M. Polansky, K. Gautschi, et al., J. Inorg. Biochem. 66 (1997) 119–130.
- [5] R.H. Matthew, G.A. Damian, S.H. Bruce, Chem. Phys. Lett. 473 (2009) 81–87.
- [6] J. Schnadt, J. Schiessling, J.N. O'Shea, S.M. Gray, L. Patthey, M.K.J. Johansson, M. Shi, J. Krempask, J.A. Ahlund, P.G. Karlsson, P. Persson, N. Martensson, P.A. Bruhwiler, Surf. Sci. 540 (2003) 39–54.
- [7] J.G. Mao, H.J. Zhang, J.Z. Ni, T.C.W. Mak, Polyhedron 17 (23–24) (1998) 3999–4009.
- [8] M.A.S. Goher, F.A. Mautner, J. Mol. Struct. 846 (2007) 153–156.
- [9] K. Franckaerts, A. Peeters, A.T.H. Lenstra, C.V. Alsenoy, Electr. J. Theory Chem. 2 (1997) 168–179.
- [10] J.R. Cobb, S.C. Percy, R.K. Gholson, J. Bacteriol. (1977) 789–794.
- [11] A. Gennaro, C.M. Sánchez-Sánchez, A.A. Isse, V. Montiel, Electrochem. Commun. 6 (2004) 627–631.
- [12] M.K. Nayak, S.K. Dogra, J. Photochem. Photobiol. A: Chem. 171 (2005) 281–290.
- [13] P.C.R. Soares-Santos, R.A. Sá Ferreira, T. Trindade, L.D. Carlos, H.I.S. Nogueira, J. Alloys Compd. 451 (2008) 575–577.
- [14] S.K. Dogra, J. Lumin. 114 (2005) 213–226.
- [15] R. Świąłocka, E. Regulska, M. Samsonowicz, W. Lewandowski, Polyhedron 28 (2009) 3556–3564.
- [16] M. Karabacak, M. Kurt, Spectrochim. Acta Part A 71 (2008) 876–883.
- [17] M. Karabacak, M. Cinar, M. Kurt, J. Mol. Struct. 885 (2008) 28–35.
- [18] M. Karabacak, M. Cinar, S. Ermeç, M. Kurt, J. Raman Spectrosc. 41 (2010) 98–105.
- [19] A.J. Dobson, R.E. Gerkin, Acta Crystallogr. C 53 (1997) 1427–1429.
- [20] A.D. Becke, J. Chem. Phys. 98 (1993) 5648–5652.
- [21] C. Lee, W. Yang, R.G. Parr, Phys. Rev. B 37 (1988) 785–789.
- [22] B.J. Orr, J.F. Ward, Mol. Phys. 20 (1970) 513–526.
- [23] N. Sundaraganesan, S. Ilakiamani, H. Saleem, P.M. Wojciechowski, D. Michalska, Spectrochim. Acta A 61 (2005) 2995–3001.
- [24] M.J. Frisch, et al., Gaussian 03 (Revision A.9), Gaussian, Inc., Pittsburgh, 2003.
- [25] J. Baker, A.A. Jarzecki, P. Pulay, J. Phys. Chem. A 102 (1998) 1412–1424.
- [26] P. Pulay, J. Baker, K. Wolinski, 2013 Green Acres Road, Suite A, Fayetteville, AR 2703, USA.
- [27] M. Karabacak, M. Kurt, J. Mol. Struct. 919 (2009) 215–222.
- [28] Y. Kwon, J. Mol. Struct. (Theochem.) 532 (2000) 227–237.
- [29] Y. Akkaya, S. Akyuz, Vib. Spectrosc. 42 (2006) 292–301.
- [30] M. Karabacak, E. Kose, M. Kurt, J. Raman Spectrosc. 41 (2010) 1085–1097.
- [31] A.R. Choudhury, T.N. Guru Row, Acta Crystallogr. E60 (2004) o1595–o1597.
- [32] M. Silverstein, G.C. Basseler, C. Morill, Spectrometric Identification of Organic Compounds, Wiley, New York, 1981.
- [33] D. Lin-Vien, N.B. Colthup, W.G. Fateley, J.G. Grasselli, The Handbook of Infrared and Raman Characteristic Frequencies of Organic Molecules, Academic Press, Boston, MA, 1991.
- [34] A. Atac, M. Karabacak, C. Karaca, E. Kose, Spectrochim. Acta A 85 (2012) 145–154.
- [35] M. Karabacak, Z. Cinar, M. Kurt, S. Sudha, N. Sundaraganesan, Spectrochim. Acta A 85 (2012) 179–189.

- [36] N. Sundaraganesan, B.D. Joshua, K. Settu, Spectrochim. Acta A 66 (2007) 381–388.
- [37] L.J. Bellamy, The Infrared Spectra of Complex Molecules, vol. 2, Chapman and Hall, London, 1980.
- [38] M. Karabacak, M. Cinar, Z. Cinar, M. Kurt, J. Mol. Struct. 982 (2010) 22–27.
- [39] A. Atac, M. Karabacak, E. Kose, C. Karaca, Spectrochim. Acta A 83 (2011) 250–258.
- [40] V. Krishnakumar, R. Ramasamy, Spectrochim. Acta A 62 (2005) 570–577.
- [41] G. Varsanyi, Assignments of Vibrational Spectra of 700 Benzene Derivatives, Wiley, New York, 1974.
- [42] G. Socrates, Infrared and Raman Characteristic Group Frequencies. Tables and Charts, 3rd ed., Wiley, New York, 2001.
- [43] N. Vijayan, R.R. Babu, R. Gopalakrishnan, P. Ramasamy, M. Ichimura, M. Palanichamy, J. Cryst. Growth 273 (2005) 564–571.
- [44] M.N. Bhat, S.M. Dharmaparakash, J. Cryst. Growth 243 (2002) 526–530.
- [45] M.S. Refat, S.A. El-Korashy, A.S. Ahmed, Spectrochim. Acta A 70 (2008) 840–849.
- [46] J.B. Lambert, H.F. Shurvell, D.A. Lightner, R.G. Cooks, Organic Struct. Spect., Simon & Schuster/A Viacom Company, New Jersey, 1998, p. 196.
- [47] M. Kumar, S. Jaiswal, R. Singh, G. Srivastav, P. Singh, T.N. Yadav, R.A. Yadav, Spectrochim. Acta A 75 (2010) 281–292.
- [48] J.O. Jensen, Vib. Spectrosc. 30 (2002) 191–195.
- [49] J.E. del Bene, J. Am. Chem. Soc. 101 (1979) 6184–6189.
- [50] N.M. O'Boyle, A.L. Tenderholt, K.M. Langer, J. Comput. Chem. 29 (2008) 839–845.
- [51] K. Fukui, Science 218 (1982) 747–754.
- [52] E.J. Behrman, R.Y. Stanui, J. Biol. Chem. 228 (1957) 923.
- [53] A.C. Testa, U.P. Wild, J. Phys. Chem. 85 (1981) 2637.
- [54] D.V.S. Jain, F.S. Nandel, P. Single, D.J. Kaur, Ind. J. Chem. 25A (1986) 15.
- [55] R.H. Abu Eittah, M.M. Hamed, A.A. Mohamed, Int. J. Quant. Chem. 64 (1997) 689–701.